Ages and geochemistry of Mesozoic-Eocene back-arc volcanic rocks in the Aysén region of the Patagonian Andes, Chile

Miguel A. Parada

Alfredo Lahsen

Departamento de Geología, Universidad de Chile, Casilla 13518, Correo 21, Santiago, Chile
maparada@cec.uchile.cl

Carlos Palacios

ABSTRACT

Eighteen new radiometric ages (fourteen ^{40}Ar-^{39}Ar, four K-Ar), combined with previously published ages, confirm the existence of three main extensional back-arc volcanic events, previously defined by stratigraphic relationships, in Chilean Patagonia (Aysén region). These three events developed during the Middle Jurassic -Early Cretaceous (160-130 Ma). Cretaceous (114-75 Ma), and Eocene (55-46 Ma). Based on distinct geochemical data and Sr-Nd isotopic characteristics of the back-arc volcanic rocks collected north and south of 46°30'S, two Mesozoic-Eocene magmatic domains are recognized: Northern Magmatic Domain (NMD) and Southern Magmatic Domain (SMD). Most analyzed basalts and intermediate volcanic rocks of the NMD have alkaline affinities and depleted to slightly depleted Sr-Nd isotopic values similar to those derived from an asthenosphere-dominated source. The SMD mafic volcanic rocks have a subalkaline character and more enriched Sr-Nd isotopic signatures, comparable to those derived from a lithospheric source. The felsic volcanic rocks of the SMD have lower εNd values and slightly higher initial $^{87}Sr/^{86}Sr$ ratios than the NMD felsic rocks, suggesting a larger crustal contribution in the magma sources. The geochemical and isotopic distinction between NMD and SMD felsic rocks could be influenced by the presence of Paleozoic metamorphic rocks as basement of the volcanic rocks of the SMD. Moreover, the compositional distinction between basalts of both domains may correspond to differences in magnitude of extension, the NMD being the one where the extension would have been greater and, consequently, the lithosphere thinner.

Key words: Back-arc volcanism, ^{40}Ar-^{39}Ar ages, Magma source, Crustal extension, Chilean Patagonia.

RESUMEN

Edades y geoquímica de las rocas volcánicas del trasarco del Mesozoico-Eoceno en la región de Aysén de los Andes patagónicos, Chile. Diez y ocho nuevas edades radiométricas (catorce ^{40}Ar-^{39}Ar, cuatro K-Ar) junto con las ya publicadas confirman la existencia de tres eventos volcánicos (previamente definidos por relaciones estratigráficas) en la Patagonia chilena (Región de Aysén) durante el intervalo Mesozoico-Eoceno: Jurásico Medio-Cretácico temprano (160-130 Ma), Cretácico (114-75 Ma) y Eoceno (55-46 Ma). Sobre la base de las características geoquímicas e isotópicas de Sr y Nd de las rocas volcánicas estudiadas, se pueden reconocer dos dominios magmáticos Mesozoico-Eoceno: Dominio Magmático Norte (DMN) y Dominio Magmático Sur (DMS). Los basaltos y rocas intermedias del DMN tienen afinidades alcalinas y valores isotópicos de Sr-Nd deprimidos a moderadamente deprimidos similares a aquellos derivados de una fuente dominada por material astenosférico. Las rocas volcánicas máficas del DMS tienen un carácter subalcalino y características isotópicas de Sr-Nd más enriquecidas comparables a aquellas derivadas de una fuente litosférica. Las rocas volcánicas félsicas del DMS tienen razones iniciales $^{87}Sr/^{86}Sr$ más altas y valores de εNd más

bajos que las rocas volcánicas félsicas de DMN, sugiriendo una mayor contribución cortical en sus fuentes magmáticas. Las distinciones geoquímicas e isotópicas entre el DMN y el DMS podrían estar influenciadas por la presencia de rocas metamórficas paleozoicas como basamento de las rocas volcánicas del DMS. Por otra parte, la distinción entre los basaltos del DMN y DMS podría corresponder a diferencias en la magnitud de la extensión, siendo el DMN donde la extensión habría sido mayor y, consecuentemente, la litósfera más delgada.

Palabras claves: Volcanismo de trasarco, Edades ^{40}Ar-^{39}Ar, Fuente magmática, Extensión cortical, Patagonia Chilena.

INTRODUCTION

The Aysén region of Patagonia is formed by three Mesozoic to Recent tectonic domains parallel to the continental margin (Fig. 1). The fore-arc domain includes mainly the southern extension of the Late Paleozoic subduction complex of central Chile (Hervé *et al.*, 1987). The westernmost part of this domain includes the area of interaction between the Chile Rise and the trench (Chile triple junction) and corresponds to the Pliocene Taitao ophiolite (cf. Nelson *et al.*, 1993). The arc domain is mainly formed by the Patagonian Batholith emplaced during the interval Late Jurassic-Late Miocene. Subduction-related active volcanoes (*e.g.*, Hudson and Maca) in this domain represent the northern limit of a volcanic gap of the Recent volcanic arc (46°30'S-49°S) as a consequence of subduction of segments of the Chile Rise (Cande and Leslie, 1986). The Liquiñe-Ofqui Fault Zone (LOFZ), active at least since the Miocene, is located along the axis of the Patagonian Batholith, and represents a major intra-arc dextral strike-slip fault system along which important displacements of the western block of the continental margin have taken place (Cembrano and Hervé, 1993). The back-arc domain, occupied by volcanic rocks and sedimentary intercalations, was formed during the Late Jurassic-Pliocene interval.

The magmatic evolution of the Aysén region has been mainly documented in the arc domain, particularly in the Patagonian Batholith where numerous studies have been undertaken in order to characterize its temporal variations (Halpern and Fuenzalida, 1978; Hervé, 1984; Bartholomew, 1984; Weaver *et al.*, 1990; Bruce *et al.*, 1991; Pankhurst and Hervé, 1994; Pankhurst *et al.*, 1999; Pankhurst *et al.*, 2000; Suárez and De La Cruz, 2001). Using different radiometric methods (Rb-Sr, K-Ar and ^{40}Ar-^{39}Ar), distinct plutonic events have been identified as responsible for the formation of the batholith. The spatial distribution of the rocks belonging to such events gives rise to an across-batholith zonation that resulted from successive intrusions within older plutons. The youngest belt (Miocene) occupies the axial zone of the batholith adjacent to the LOFZ (Hervé, 1984; Pankhurst and Hervé, 1994). To the east of the axial zone, Cretaceous plutons were assembled forming the widest plutonic belt of the batholith, whereas westward from the axial zone, Early Cretaceous-Eocene intrusions have been identified (Bartholomew, 1984; Bartholomew and Tarney, 1984; Pankhurst *et al.*, 1999) forming poorly defined belts. Eastern satellite plutons of jurassic ages have been recognized (Parada *et al.*, 1997; Pankhurst *et al.*, 2000; Suárez and De La Cruz, 2001). The lack of a regular unidirectional migration of the Meso-Cenozoic intrusions with time contrasts with the eastward migrating Meso-Cenozoic belts developed in the Andes of central Chile (cf. Drake *et al.*, 1982; Parada *et al.*, 1988), and suggests a plutonic development in a more stationary condition.

The back-arc evolution of Andean Patagonia has been the subject of several studies. Most of them are concerned with the Mesozoic stratigraphy of the area between Coyhaique and Lake General Carrera (cf. A. Lahsen[1]; Skármeta and Charrier, 1976; Suárez and De la Cruz, 1997), along with Neogene volcanism, sedimentation and deformation recognized south of Lake General Carrera (*e.g.*, Niemeyer *et al.*, 1984; Suárez and De La Cruz, 2000; Suárez *et al.*, 2000) processes whose association with the collision and subduction of segments of the Chile Ridge at that time is controversial (*e.g.*, Charrier *et al.*, 1979; Ramos and Kay, 1992; Petford and Turner, 1993; Flint *et al.*, 1994; Suárez *et al.*, 2000). Based on published and new

[1] 1966. Geología de la región continental de Aysén (Unpublished Report), *Instituto de Investigaciones de Recursos Naturales, Corporación de Fomento de la Producción*, 25 p. Santiago.

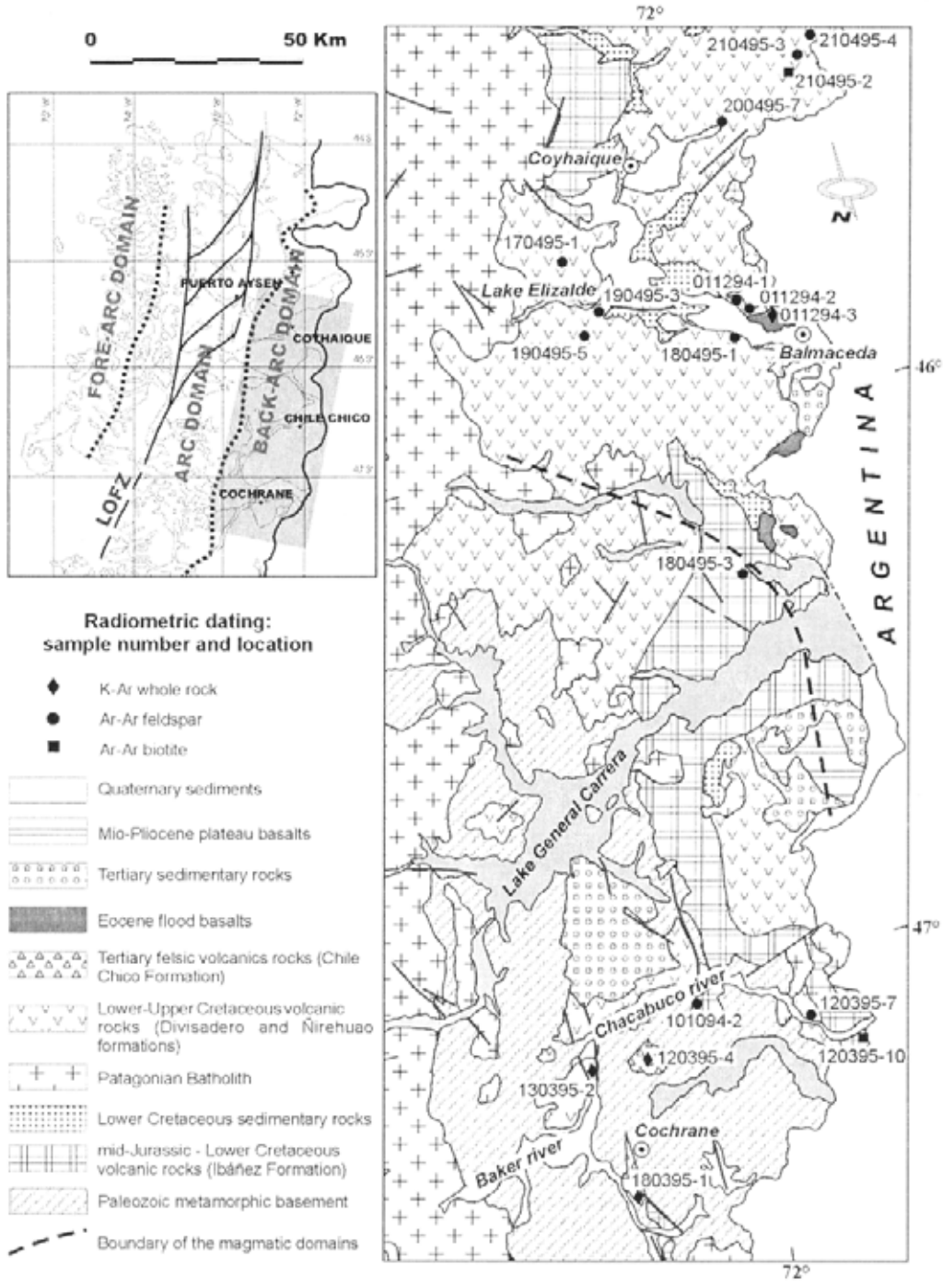

FIG. 1. Geological map of the back-arc domain of the Aysén region. Source of information: A. Lahsen[1]; Niemeyer (1975); Yoshida (1981); A. Lahsen, C. Palacios, M.A. Parada, G. Sánchez, B. Townley and J. Villegas[2]; M.Suárez and R. De la Cruz[3], and this study. Insert: main part of the Aysén Region, location of the studied area (shaded), and distribution of the tectonic domains. LOFZ: Liquiñe-Ofqui Fault Zone.

[2] 1994. Exploración geoquímica estratégica en la Región de Aysén. Proyecto FONDEF MI-15 (Unpublished Report), *Universidad de Chile, Departamento de Geología*, 367 p.

[3] 1994. Geología de la parte oriental de las Hojas Puerto Cisnes, Coyhaique y Chile Chico (Unpublished Report), *Servicio Nacional de Geología y Minería*, 386 p.

ages (mineral ^{40}Ar-^{39}Ar and whole-rock K-Ar ages). This study is a contribution to a better understanding of the Mesozoic-Eocene volcanic history in the Aysén region, including ^{40}Ar-^{39}Ar results obtained in back-arc volcanic sequences. Particularly relevant are the geochronological results on volcanic rocks south of Lake General Carrera, where the available radiometric ages are less abundant. Furthermore, this study presents the geochemical and Sr-Nd isotopic characteristics of some rocks of the studied back-arc segment. Based on these characteristics the authors distinguish two north-south magmatic domains. The role of lithosphere and asthenosphere with respect to the origin of the compositional characteristics of the two domains is discussed.

ANALYTICAL METHODS

Mineral separates from fourteen samples were analyzed by using the ^{40}Ar-^{39}Ar technique at the Geochronology Laboratory, Stanford University. Plagioclase and biotite separates were packaged in 99.999% pure copper foil packets. The packets were interspersed in a pure quartz-glass tube with aluminum foil packets containing 10-20 grains of sanidine standard 85G003 from the Taylor Creek Rhyolite (TCR). used as a neutron fluence monitor. The age of the TCR sanidine is taken to be 27.92 Ma (Duffield and Dalrymple 1990). Groups of 2-4 sanidine grains were fused using a Spectra-Physics 2016 Ar ion laser operating in all-lines mode at a nominal output power of 6W. Prior to measurement, each sample was introduced into the resistance furnace and degassed at 400°C or 450°C to release much of the contaminating atmospheric argon; this gas fraction was not analyzed. Complete ^{40}Ar-^{39}Ar release spectra and apparent ages (± 1 σ uncertainty) are given in figures 2, 3 and 4.

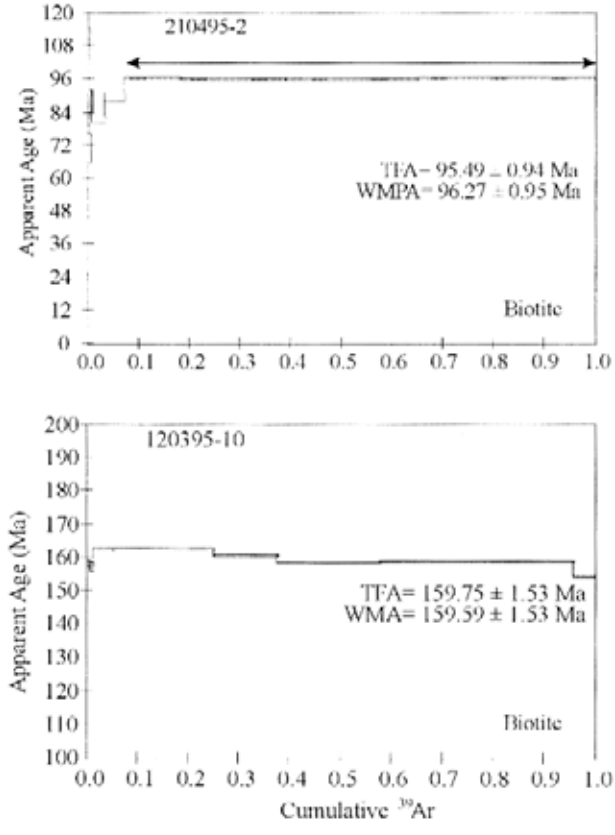

FIG. 2. ^{40}Ar-^{39}Ar release spectra measured for biotites. The solid steps within the release spectra indicate the increments used for calculating weighted mean ages. TFA: total fusion age; WMPA: weighted mean plateau age; WMA: weighted mean age.

The decay constants used in the K-Ar age determinations are: $\lambda_e = 0.581 \times 10^{-10}$ yr^{-1}, $\lambda_\beta = 4.962 \times 10^{-10}$ yr^{-1}. The value of $^{40}K/K$ used for age calculation is 0.01167±0.00004. K-Ar age determinations were obtained at the Geochronological Laboratory of SERNAGEOMIN (Servicio Nacional de Geología y Minería).

The whole-rock chemical analyses were obtained by ICP-AES at the Department of Geology, University of Chile, and by atomic absorption at SERNAGEOMIN. The Sr and Nd isotope data were obtained at Geochron Laboratories. The rock powder was dissolved in $HF+HNO_3$. Sr and Nd were isolated by ion exchange and analyzed. The Sr analyses are normalized to $^{87}Sr/^{86}Sr = 0.11940$. Analyses of NBS 987 averaged 0.710241 (± 0.000014) (n=60) during the period of these analyses. The Nd analyses are normalized to $^{146}Nd/^{144}Nd=0.7219$. Analyses of La Jolla Nd averaged 0.511852 (± 0.00010) (n= 60) during the period of these analyses. Errors on $^{87}Sr/^{86}Sr$ and $^{143}Nd/^{144}Nd$ are given as 2σ (95%) in the last two digits (Table 5).

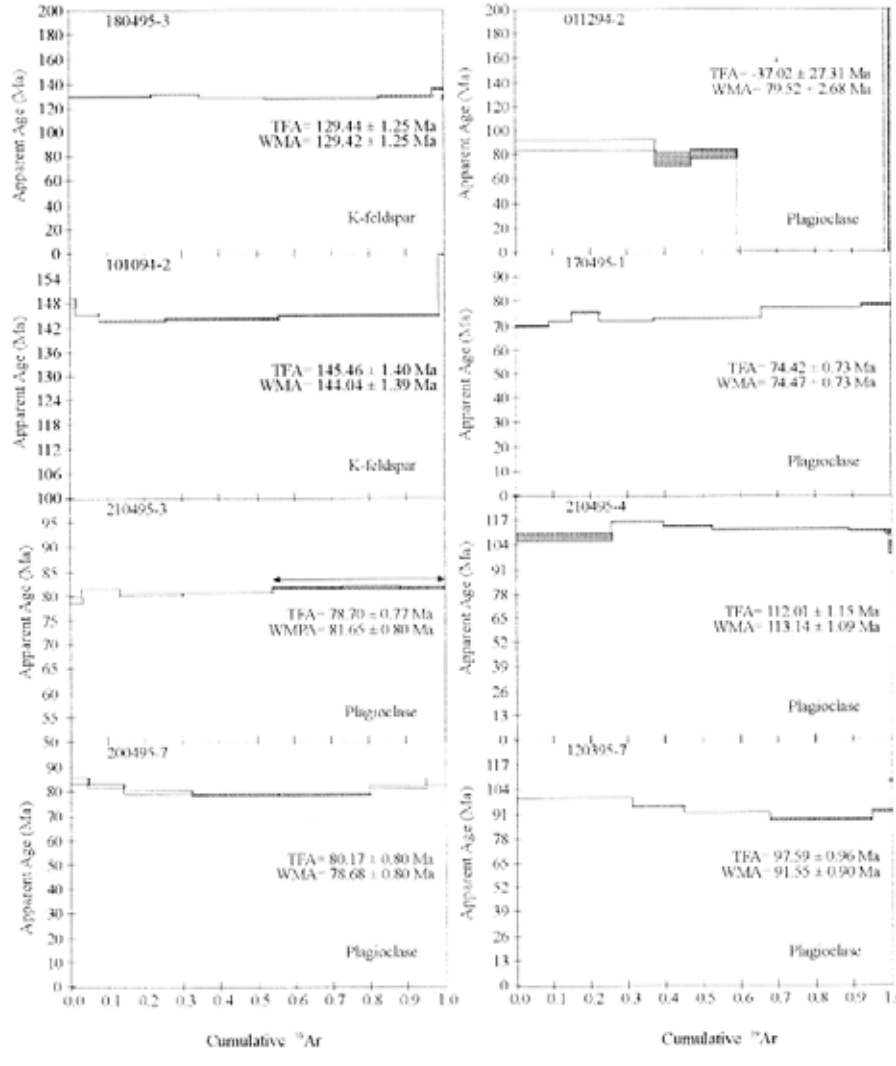

FIG. 3. Representative ^{40}Ar-^{39}Ar release spectra measured for K-feldspars and plagioclase. The solid steps within the release spectra indicate the increments used for calculating weighted mean ages. Abbreviations are as in figure 2. The remainder ^{40}Ar-^{39}Ar spectra are available from the authors on request.

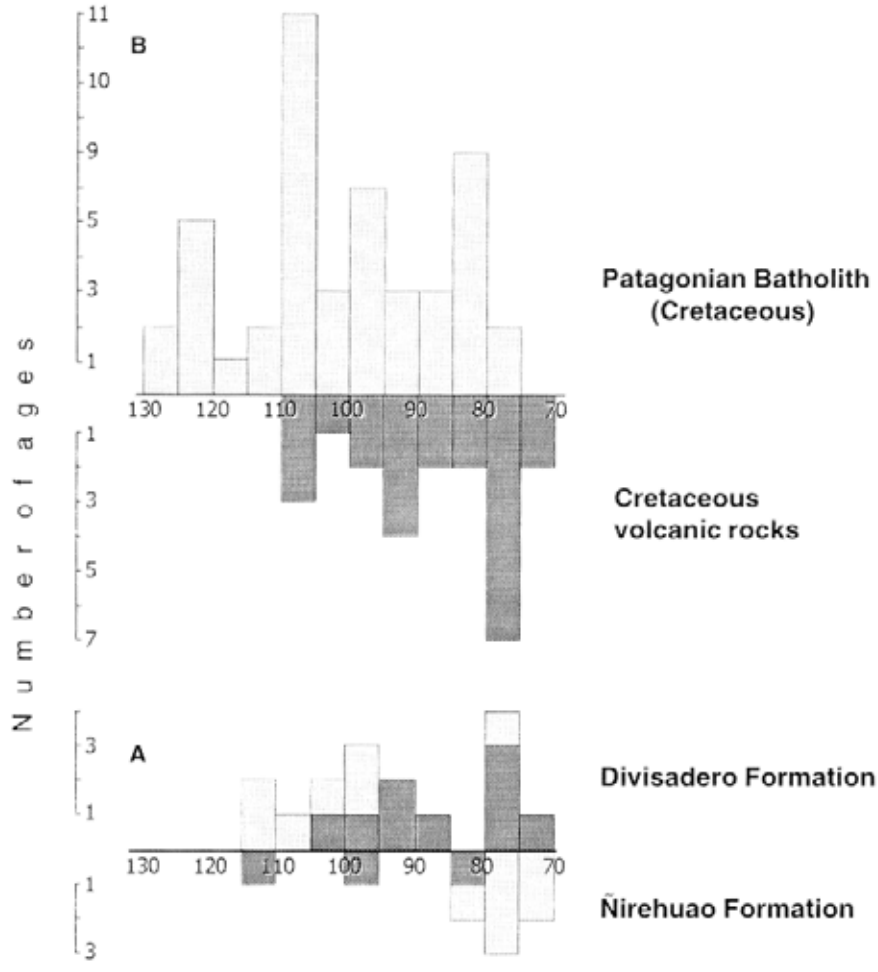

FIG. 4. **A-** Histograms with ages of the Divisadero and Ñirehuao Formations; darker bars indicate the new radiometric data given here; **B-** Histograms of Cretaceous ages of rocks of the Patagonian Batholith and back-arc volcanic rocks between 45 and 48°S. Published data were compiled from Weaver *et al.* (1990); Pankhurst and Hervé (1994); M. Suárez and R. De la Cruz (1994)[3]; Belmar (1996) and Pankhurst *et al.* (1999).

GEOLOGICAL SETTING AND SAMPLE PROVENANCE FOR THE RADIOMETRIC DATES

Most of the stratigraphic relationships known in the back-arc area of the Aysén region have been established north of Lake General Carrera. In order to provide geochronological support to the stratigraphic framework and extend further south the knowledge of the evolution of this back-arc segment, the dated samples were collected in two areas: between Coyhaique and Balmaceda (45° 30' - 46°S) and along the Chacabuco river (47-47°30'S) (Fig. 1).

The volcanic rocks studied here developed to the east of the Patagonian Batholith, as a result of a Meso-Cenozoic back-arc extensional regime (Bartholomew and Tarney, 1984) the products of which were draped over a highly deformed Upper Paleozoic metamorphic basement cropping out south of Lake General Carrera (46°S). During the volcanic evolution, two marine incursions interrupted continental sedimentation. The oldest corresponds to the Late Jurassic - Early Cretaceous basin (Aysén

Basin), which was filled by the transgressive - regressive succession of the Coyhaique Group, composed of coral reef and bioclastic limestones, black shales, and marine-continental sandstones and conglomerates (Cotidiano, Katterfeld and Apeleg formations, respectively; Ramos, 1976; Bell and Suárez, 1997). The younger sedimentary interval corresponds to a spatially restricted Late Oligocene-Miocene sedimentary basin (Cosmelli Basin; Flint *et al.*, 1994; Suárez *et al.*, 2000) that formed inboard of the Chile triple junction (47°S). The Tertiary deposits overlie the metamorphic basement and Mesozoic volcanoclastic strata and represent a stratigraphic succession of continental and marine facies resulting from marked base level changes (Flint *et al.*, 1994).

A Jurassic volcanic belt is exposed between 43° and 50°S near the Chile-Argentina border. It includes sequences of acidic to intermediate volcanic rocks (Ramos *et al.*, 1982). In the studied area, the Jurassic event is represented by felsic volcanic sequences (here referred to as the Ibáñez Formation) underlying the marine sequence of the Early Cretaceous Coyhaique Group, and deposited over Paleozoic metamorphic rocks in the region south of Lake General Carrera. The Ibáñez Formation forms part of the Jurassic large igneous province of Patagonia, which is one of the largest silicic provinces on Earth (Féraud *et al.*, 1999). Three samples of rhyolitic tuffs from the Ibáñez Formation were dated. One of them (sample 180495-3) was collected near Levicán Peninsula on the northeastern shore of Lake General Carrera (46°30'S). The other two samples (120395-10 and 101094-2) were taken at the Chacabuco River, south of Lake General Carrera.

The Cretaceous volcanism appears to be the most intensive, as is suggested by the extension of its exposures, and is represented by volcanic rocks of the Divisadero and Ñirehuao formations (cf. Skármeta and Charrier, 1976). The Divisadero Formation overlies the Ibáñez Formation or the marine sedimentary rocks of the Coyhaique Group (Berriasian-Barremian; cf. M. Suárez and R. De la Cruz,[3]; Belmar, 1996) and is in faulted contact with the Ñirehuao Formation that crops out east of Coyhaique. It is composed mainly of felsic tuffs and lavas, with a minor amount of flat-lying basaltic rocks. Continental sedimentary rocks are locally interbedded with the volcanic strata. The Ñirehuao Formation mainly occurs in the eastermost part of the Coyhaique and Ñirehuao River basins and is lithologically similar to the Divisadero Formation, although it contains a larger amount of basaltic rocks. Although the stratigraphic position of both formations is similar, the observed lithological differences between them correspond to their different position with respect to the plutonic arc: the Divisadero Formation developed between the arc-related Patagonian Batholith and the eastern back-arc position, where the Ñirehuao Formation was deposited.

Eight samples from the Divisadero Formation were dated. Six of them were collected south of Coyhaique, in the vicinity of Lake Elizalde and Balmaceda (Fig. 1). They represent three felsic rhyolitic tuffs (011294-2, 170495-1, 180495-1), two basalt flows (011294-1 and 190495-3) and a gabbro (190495-5) hosted in volcanic rocks of Divisadero Formation. The remaining two samples were collected at widely separated localities along the Chacabuco River (Fig. 1), and include a dacitic tuff (120395-7) and a fragment of a rhyolite pumice (130395-2) of a felsic tuff. Four samples from the Ñirehuao Formation were dated and represent a rhyolitic tuff (210495-2), two andesites (200495-7 and 210495-3) and a basalt (210495-4) that were collected from a flat-lying volcanic sequence at the Coyhaique River, near the Argentina-Chile boundary (Fig. 1).

The Tertiary volcanic event is represented mainly by the volcanic products of Chile Chico Formation (Niemeyer, 1975) south of Lake General Carrera, by an Eocene sequence of olivine-phyric flood basalts outcropping near Balmaceda at 45°45'S (cf. Demant *et al.*, 1996), and by the lower flood basalts of the westward extension of the larger Eocene- Pliocene Meseta Buenos Aires (Charrier *et al.*, 1979; Petford *et al.*, 1996) developed south of Chile Chico village (*ca.* 46°30'S). These basalts correlate with the Eocene Posadas flood basalts (Ramos and Kay, 1992) located in the Argentinian Patagonia within the latitudes of the Recent arc volcanic gap. The Posadas basalts have been considered to be related to the subduction of part of the Aluk-Farallón ridge beneath the continental margin during the Eocene (cf. Ramos and Kay, 1992). A sample (011294-3) from the Balmaceda flood basalts and two rhyolitic tuffs (120395-4, 180395-1) of Chile Chico Formation were dated.

TABLE 1. SUMMARY OF THE ^{40}Ar-^{39}Ar RESULTS.

Sample	Rock type	UTM Coordinates	Mineral dated	Number of steps	Age range of steps (Ma) ± 1 σ	TFA* (Ma)	WMA** (Ma)	WMPA*** (Ma)	Preferred age (Ma)
Ibáñez Formation									
180495-3	Rhyolitic tuff	4867480N 271156E	K-feldspar	7	187.9 ± 1.2 - 135.4 ± 1.3	129.4 ± 1.3	129.4 ± 1.3		129 ± 1.0
101094-2	Rhyolitic tuff	4784034N 701634E	K-feldspar	7	144.0 ± 1.4 - 279.4 ± 11.8	145.5 ± 1.4	144.0 ± 1.4		144 ± 1.0
120395-10	Rhyolitic tuff	4772000N 728000E	Biotite	8	154.6 ± 1.5 - 162.6 ± 1.6	159.8 ± 1.5	159.6 ± 1.5		160 ± 2.0
Divisadero Formation									
180495-1	Rhyolitic tuff	4916674N 278253E	Plagioclase	7	87.0 ± 0.9 - 112.8 ± 1.1	100.2 ± 1.0	87.0 ± 0.9		87 ± 1.0
011294-1	Basaltic andesite	4920160N 279800E	Plagioclase	5	74.7 ± 2.3 - 173.0 ± 119.6	107.0 ± 1.9	74.8 ± 2.3		75 ± 2.0
190495-5	Norite	4919995N 712655E	Plagioclase	7	98.3 ± 1.0 - 118.4 ± 1.2	107.3 ± 1.1	98.3 ± 1.0		98 ± 1.0
120395-7	Dacitic tuff	4772028N 712507E	Plagioclase	7	91.5 ± 0.9 - 118.5 ± 4.7	97.6 ± 1.0	91.6 ± 0.9		92 ± 1.0
011294-2	Rhyolite tuff	4919844N 282618E	Plagioclase	7	76.3 ± 5.4 - 88.0 ± 4.0		79.5 ± 2.7		79.5 ± 2.7
190495-3	Basalt	4924862N 716933E	Plagioclase	7	97.0 ± 1.0 - 135.0 ± 1.8	110.2 ± 1.1	99.5 ± 1.0		99 ± 1.0
170495-1	Rhyolitic tuff	4936830N 711690E	Plagioclase	7	73.2 ± 0.7 - 78.5 ± 0.8	74.4 ± 0.7	74.5 ± 0.7		74 ± 1.0
Ñirehuao Formation									
210495-2	Rhyolitic tuff	4967275N 300249E	Biotite	9	71.1 ± 4.9 - 99.2 ± 15.1	95.5 ± 0.9		96.3 ± 1.0	96.3 ± 1.0
210495-3	Andesite	4968417N 300037E	Plagioclase	7	79.3 ± 0.9 - 81.8 ± 0.8	78.7 ± 0.8		81.7 ± 0.8	82 ± 1.0
200495-7	Andesite	4954900N 279480E	Plagioclase	7	78.7 ± 0.8 - 84.4 ± 1.4	80.2 ± 0.8	78.7 ± 0.8		78 ± 1.0
210495-4	Olivine basalt	4972324N 302012E	Plagioclase	7	102.3 ± 3.4 - 116.6 ± 1.1	112.0 ± 1.2	113.1 ± 1.1		112 ± 1.0

*TFA: Total Fusion Age

**WMA: Weighted Mean Age

***WMPA: Weighted Mean Plateau Age

GEOCHRONOLOGICAL RESULTS

The chronological results were obtained from eighteen pre-Miocene rock samples: ten ^{40}Ar-^{39}Ar dates on plagioclase, two ^{40}Ar-^{39}Ar on K-feldspar, two ^{40}Ar-^{39}Ar on biotite, and four whole-rock K-Ar (see Tables 1 and 2). A limitation concerning the criteria of selection of samples and the interpretation of chronological data given here is the regional scale presence of secondary minerals product of very low grade metamorphism of the studied volcanic sequences (Table 3, cf. Aguirre *et al.*, 1997). This can be particularly relevant in the interpretation of some ages obtained on feldspars.

BIOTITE ^{40}Ar-^{39}Ar RESULTS

Biotites from samples 210495-2 and 120395-10 were analyzed. The Ar spectra are shown in figure 2. The first sample yielded a flat release spectrum with a plateau age of 96.3± 1.0 Ma, consistent with the age of the Ñirehuao Formation from which it was collected. The second sample has an excess Ar spectrum; however the total fusion age (TFA) of 159.8±1.5 Ma and the weighted mean age (WMA) of 159.6 ±1.5 Ma are consistent with the age assigned to the Ibáñez Formation from which it was taken.

FELDSPAR ^{40}Ar-^{39}Ar RESULTS

K-feldspar from samples 180495-3 and 101094-2 do not exhibit a plateau in the ^{40}Ar-^{39}Ar spectrum (Fig. 3). Both samples were taken from the Ibáñez Formation. For the first sample the TFA and WMA are identical (129.4±1.3 Ma). The TFA and WMA ages of the second sample do not differ substantially; the authors prefer the WMA of the two youngest steps (144.0±1.0 Ma).

Most of the ten ^{40}Ar-^{39}Ar spectra for plagioclase exhibit shapes of excess Ar or are irregular (Fig. 4). The exception is sample 210495-3, which shows a plateau only in the last 3 steps. Considering these steps, which make up <50% of the gas, a weighted mean age of 81.7±0.8 Ma is obtained. Samples 200495-7, 120395-7 (Fig. 3), 180495-1 and 190495-5 have typical excess Ar spectra and yield significant differences between the TFA and the WMA. In all these cases the age could be close to WMA (78.7±0.8, 87.0±0.9 Ma, 98.3±1.0 Ma and 91.6±0.9 Ma for the samples listed above). Plagioclase from sample 011294-1 released almost no gas, although both TFA and WMA (Table 1) are consistent with the age of the Divisadero Formation from which it was taken. Sample 011294-2 is unusual in that two of the high temperature steps released a lot of atmospheric gas (Fig. 3). The WMA of the middle two steps (79.5±2.7) is preferred. The spectrum of sample 190495-3 (not shown) is also unusual because every step is internally discordant. The resulting TFA and WMA are 110.2±1.1 Ma and 99.5±1.0 Ma, respectively, although the inverse isochron of the first three points gives a more reliable age of about 99 Ma. Despite the fact that sample 170495-1 has a small excess Ar spectrum, and sample 210495-4 (Fig. 3) has a slightly disturbed Ar spectrum, both samples do not show differences between TFA and WMA, indicating that the real ages are close to 74 Ma and 112 Ma, respectively.

WHOLE-ROCK K-Ar RESULTS

Four samples of volcanic rocks were dated (Table 2). Sample 011294 was taken from the Balmaceda flood basalts. The age of 49.0±2.1 Ma is consistent with two previous whole-rock K-Ar ages of 46 and 55 Ma (Baker *et al.*, 1981; Butler *et al.*, 1991). Sample 130395-2 was dated at 104±3.0 Ma and corresponds to a ~7 cm long pumice fragment collected from a rhyolitic tuff of the Cretaceous Divisadero Formation. The remaining two samples

TABLE 2. K-Ar WHOLE-ROCK AGE DATA FOR VOLCANIC ROCKS.

Sample	Rock type	UTM Coordinates	wt.% K	^{40}Ar rad (nl/g)	% Atm Ar	Age (Ma) ± (2σ)
130395-2	Rhyolitic tuff	4779620N 680033E	3.560	14.86	10	104.0 ± 3.0
011294-3	Olivine basalt	4917763N 287069E	0.723	1.4	46	49.0 ± 2.1
120395-4	Rhyolite tuff	4777920N 691120E	3.668	6.77	9	46.8 ± 1.5
180395-1	Rhyolitic tuff	4757466N 681644E	2.418	4.48	11	47.0 ± 1.6

TABLE 3. SUMMARY OF PETROGRAPHIC FEATURES AND SECONDARY MINERALOGY OF THE DATED SAMPLES.

Sample	Rock type	Mineral components	Observation/Alteration
Ibáñez Formation			
180495-3	Rhyolitic tuff	**CF** (37%): Qz, K-feld, Ab; **LF** (3%): Mf,Vf; **GM** (60%): ash	clays +/- carbonates in Alk-feld
101094-2	Rhyolitic tuff	**CF** (18%): Qz, K-feld, Ab; **GM** (82%): ash	unaltered Alk-feld
120395-10	Rhyolitic tuff	**CF** (35%): Qz, Alk-feld, Bt; **GM** *(65%)*: glass	Bt slightly oxidized
Divisadero Formation			
180495-1	Rhyolitic tuff	**CF** (15%): Pl, Qz; **LF** (2%): Vf; **GM** (83%): ash	Pl slightly argillic
011294-1	Basaltic andesite	**Ph** (3%): Pl, Ol; **GM** (97%): Pl, Mt	Pl partially argillic; bowlingite replacing Ol
190495-5	Norite	**Pl** (90%). Opx (10%)	unaltered Pl cumulates
120395-7	Rhyolitic tuff	**CF** (40%): Pl, Qz, Bt, Mt; **GM** (60%): ash	unaltered Pl, Bt slightly chloritized
011294-2	Dacitic tuff	**CF** (10%): Pl, Qz; **GM** (90%): ash	Pl partially argillic
190495-3	Basalt	**Ph** (10%): Pl, Cpx, Opx, Ol; **GM** (90%): Pl, Mt	clays + chlorite in Pl, bowlingite in Opx and Ol
170495-1	Rhyolitic tuff	**CF** (35%): Qz, Pl, K-feld, Bt; **GM** (65%): ash	feldspar partially argillic, Bt slightly chloritized
130395-2	Rhyolitic tuff	**CF** (40%):Qz, Pl, Bt; **GM** (60%): ash	Pl slightly argillic, Bt slightly choritized
Ñirehuao Formation			
210495-2	Rhyolitic tuff	**CF** (7%): Qz, Bt; **GM** (93%): ash	unaltered Pl and Bt
210495-3	Andesite	**Ph** (35%): Pl, Opx; **GM** (65%): glass, Pl	unaltered Pl
200495-7	Andesite	**Ph** (25%): Pl, Cpx; **GM** (75%): glass, Pl	unaltered Pl
210495-4	Olivine basalt	**Ph** (20%): Cpx, Ol, Pl; **GM** (80%): Pl, Cpx, Mt	Pl partially chloritized
Balmaceda basalts			
011294-3	Olivine basalt	**Ph** (5%): Ol, Opx; **GM** (95%): Pl, Mt,	iddingsite partially replacing Ol
Chile Chico Formation			
120395-4	Rhyolitic tuff	**CF** (30%): Qz, Alk-feld; **LF** (3%): Mf; **GM** (67%): glass	Alk-feld slightly replaced by carbonates
180395-1	Rhyolitic tuff	**CF** (10%): Qz, Alk-feld, **LF** (2%): **GM** (88%): ash	Alk-feld replaced by carbonates and clay minerals

CF: crystal fragment
LF: lithic fragment (Vf, Mf: volcanic, metamorphic)

GM: groundmass
Ph: phenocryst

correspond to rhyolitic tuffs (120395-4 and 180395-1) that were taken from a sequence tentatively assigned to the Chile Chico Formation. The ages obtained (~47 Ma) are Eocene, similar to the age of the Balmaceda basalts.

STRATIGRAPHIC IMPLICATIONS OF THE GEOCHRONOLOGICAL DATA

Previous age data of the back-arc volcanic rocks and the eighteen new radiometric dates given here, roughly confirm the magmatic events identified by Suárez and De la Cruz (1997; 2001) using the available radiometric data including both arc plutonic and back-arc volcanic rocks of the northern part of Aysén. The pre-Miocene volcanic events defined in this study are: Middle-Jurassic-Early Cretaceous (160-130 Ma), Cretaceous (114-75 Ma), and Eocene (55-46 Ma).

At the Levicán Peninsula, on the northeastern shore of Lake General Carrera (~ 46°30'S), a rhyolitic tuff (sample 180495-3), from a typical sequence of the Ibáñez Formation, gave an ^{40}Ar-^{39}Ar WMA on K-feldspar of 129.4±1.2 Ma, which is younger than the assigned Jurassic age of this formation. The age obtained here is also younger than a U-Pb zircon age of 153.0±1.0 Ma (Pankhurst *et al.*, 2000). A depletion of radiogenic ^{40}Ar in the analysed feldspar after very low-grade metamorphic reequilibration can be responsible of the younger age. Rocks of the Jurassic event were confirmed along the Chacabuco River. The ages of 144.0±1.4 Ma (sample 101094-2) and 159.6±1.5 Ma (sample 120395-10) are consistent with the ^{40}Ar-^{39}Ar age of 130±2 Ma obtained from a quartz-dioritic porphyry stock hosted by the Ibáñez Formation, exposed in the eastern part of the Chacabuco Valley (Townley, 1996). In addition, the Jurassic event has been documented in the El Faldeo polymetallic district (south of Cochrane), where tonalite plutons have been dated (Parada *et al.*, 1997) at 155±10 Ma (U-Pb in zircons) and ~158±1.5 Ma (^{40}Ar-^{39}Ar for biotites). Whole-rock K-Ar age determinations of pervasively sericitized felsic rocks of this district indicate alteration ages between 142 and 140 Ma (Palacios *et al.*, 1997).

It is interesting to note that the jurassic ages obtained here confirm the trend of decreasing ages from ENE (*ca.*190 Ma) to the WSW (144 Ma) of the Jurassic large igneous province of Patagonia (Féraud *et al.*, 1999).

The eight new ages of the Divisadero Formation (seven ^{40}Ar-^{39}Ar plagioclase, and one K-Ar whole-rock dating; Tables 1 and 2) fall in the broad range 74.0±1.0 to 104.0±3.0 Ma. The ages of samples taken from the Ñirehuao Formation (40-50 km northeast of Coyhaique, Fig. 1) reported here cover even a broader range (78±1.0-112±1.0 Ma; Table 1) and partially overlap those published Late Cretaceous K-Ar ages obtained in neighbouring localities such as Morro Negro (71-81 Ma; Baker *et al.*, 1981; Butler *et al.*, 1991).

The age determinations available for the Divisadero and Ñirehuao formations (twelve previous K-Ar and Rb-Sr ages, and eleven new ^{40}Ar-^{39}Ar mineral ages) indicate that the Cretaceous volcanic evolution took place during the Albian-Campanian interval (115-75 Ma; Fig 4a) with an apparent peak in the Late Cretaceous. The Cretaceous volcanism would have started at a later time with respect to the Cretaceous plutonic history (mainly determined by K-Ar ages; Fig. 4b). Since K-Ar and ^{40}Ar-^{39}Ar dates are cooling ages below temperatures of Ar retention in potassium-bearing phases, the differences in ages between the onset of plutonism and volcanism, should be larger than those shown in figure 4b. Cretaceous volcanogenic Au mineralization has been recognized through a sericite ^{40}Ar-^{39}Ar age of about 80 Ma obtained from an altered felsic volcanic rock sample of the upper section of the Divisadero Formation sequence exposed at the junction of the Chacabuco and Baker rivers (C. Palacios, A. Lahsen, M.A. Parada and R. Townley)[4].

The Balmaceda flood basalts have consistent Eocene ages (46-55 Ma), which are similar to the Eocene ages of the lower section of the Meseta Buenos Aires flood basalts (Charrier *et al.*, 1979; Petford *et al.*, 1996). A hiatus in the volcanism of

[4] 1997. Carta metalogénica de la región oriental de Aysén (Unpublished Report), *Universidad de Chile-Gobierno Regional XI Región*, 112 p.

nearly 20 my is apparent from the difference in age between the youngest Late Cretaceous volcanic rocks and the oldest Eocene basalts. This interval corresponds to a period of extremely oblique convergence (or divergence) between the Farallón and South American plates (cf. Pardo-Casas and Molnar, 1987).

GEOCHEMICAL CHARACTERISTICS: DEFINITION OF TWO MAGMATIC DOMAINS

A geochemical database of new 32 major and trace element analyses were used to characterize the composition of the studied volcanic rocks. Major and trace element compositions of rocks belonging to the Jurassic, Cretaceous and Eocene volcanic events are given in table 4. Only felsic volcanic rocks have been recognized in the Jurassic event of the studied area. However, further east in Argentina, Ramos (1976) described andesitic lavas and tuffs as the main constituents of the Jurassic La Plata Formation. The two youngest events are characterized by a bimodal association of abundant tuffs and lavas of rhyolitic and dacitic composition, and a minor amount of basaltic and andesitic lavas.

The Sr and Nd isotope data in table 5 were obtained from 16 representative samples (10 felsic tuffs and 6 basalts, basaltic andesites and andesites). With the exception of the highly anomalous sample 180395-1, the initial $^{87}Sr/^{86}Sr$ ratios of the analyzed samples fall in the range of 0.704-0.712 with the felsic volcanic rocks being the most radiogenic. The εNd values for the whole set of samples range from +5.1 to -4.7.

In the following sections the authors will emphasize the differences between the geochemical and Sr-Nd isotopic compositions of the Mesozoic-Eocene rocks collected around the Coyhaique-Balmaceda area and those collected in the Chacabuco Valley- Cochrane area. Such differences allow the recognition of two magmatic domains: a Northern Magmatic Domain (NMD) and a Southern Magmatic Domain (SMD).

One of the most distinct geological features of the SMD is the presence of a huge Paleozoic metamorphic massif. This massif served as a bridge between two large north-south Mesozoic basins that have been recognized along the southernmost Andean segment (Aysén and Austral Basins; cf. Bell and Suárez, 1997). It was exposed to erosion before the onset of the Mesozoic volcanism, as indicated by the presence of abundant metamorphic rock fragments in basal conglomerates of the Ibáñez Formation of the SMD. This situation, together with the participation of the Paleozoic metamorphic rocks in the origin of the SMD Mesozoic volcanic rocks and associated mineralization (see below) explains the location of the domain boundary proposed here (Fig. 1) that roughly coincides with the latitude of the northernmost exposures of the metamorphic massif (Río Lácteo Formation; Bell and Suárez, 2000).

NORTHERN MAGMATIC DOMAIN (NMD)

Most of the basalts of the NMD have alkaline affinities (Fig. 5a) and include some primitive basalts (wt.% MgO: 6.6 and 8.3) with the highest La/Yb ratios (Fig. 5b). The spider diagram of trace element compositions (normalized to N-MORB) of representative Lower Cretaceous, Upper Cretaceous and Eocene basalts of the NMD collected near Balmaceda and neighbouring areas, shows similar trends. However, only the Lower Cretaceous basalt exhibits the Nb depletion commonly observed in subduction-related rocks, and the Eocene basalt shows the largest Nb enrichment (Fig. 6) suggesting a progression from an arc-like source to OIB source during the Lower Cretaceous-Eocene interval.

The analyzed NMD basalts, basaltic andesites and andesites show considerable variations in initial $^{87}Sr/^{86}Sr$ ratios and in εNd (Sr_i: 0.70397 to 0.70578; εNd: +0.1 to +4.9), however, they are isotopically depleted, with the Eocene Balmaceda basalt being the most depleted one (Table 5). Although different degree of crustal contribution cannot be ruled out to explain the observed Sr-Nd isotopic variations, all the NMD mafic volcanic rocks fall within the field of modern OIB (cf. Feuerbach *et al.*, 1993) (Fig. 7), suggesting the participation of asthenospheric components in the source. A similar conclusion was reached by Demant *et al.* (1996) who considered

TABLE 4. CHEMICAL ANALYSES OF REPRESENTATIVE MESOZOIC - EOCENE VOLCANIC ROCKS FROM THE BACK-ARC DOMAIN OF THE AYSEN REGION. MAJOR AND TRACE ELEMENTS COMPOSITIONS IN WT.% AND PPM, RESPECTIVELY.

	Jurassic					Cretaceous										
Sample	180495-2	180495-3	180495-4	120395-10	210495-4	190495-1	190495-3	011294-1	210495-3	120395-7	200495-7	180495-1	200495-6	210495-5	190495-6	200495-1
SiO2	63.97	74.40	74.85	74.94	48.24	48.54	52.77	54.40	61.28	61.14	62.03	64.78	67.50	68.17	75.30	74.92
TiO2	1.04	0.20	0.14	0.17	1.17	1.37	0.99	1.68	0.80	0.40	0.64	0.65	0.17	0.56	0.21	0.13
Al2O3	15.23	13.37	13.10	13.09	15.95	20.58	17.22	17.50	17.14	15.48	15.61	16.18	16.05	15.01	13.25	12.49
Fe2O3	7.04	1.65	0.76	1.96	3.27	3.73	2.84	5.26	1.92	1.95	1.96	4.29	0.72	3.12	0.94	0.96
FeO	0.28	0.32	0.76	0.25	5.28	4.00	5.46	3.16	3.36	1.55	2.76	0.42	1.00	0.38	1.34	0.42
MnO	0.05	0.03	0.04	0.02	0.18	0.28	0.18	0.35	0.12	0.20	0.08	0.06	0.08	0.04	0.07	0.02
MgO	0.42	0.42	0.38	0.20	8.29	3.35	4.79	2.40	2.59	0.98	2.48	0.26	0.93	0.88	0.49	0.43
CaO	0.79	0.64	0.86	0.16	9.20	6.66	8.24	2.10	5.38	6.01	4.70	1.07	2.35	2.60	0.97	0.64
Na2O	6.15	3.19	4.61	1.46	2.76	4.35	3.00	5.97	4.10	2.44	3.35	6.14	4.30	4.36	3.29	1.77
K2O	2.92	4.67	2.72	4.79	2.05	1.49	1.22	3.05	1.62	4.88	1.91	4.87	4.20	3.18	5.14	5.99
P2O5	0.32	0.03	0.02	0.02	0.27	0.46	0.20	0.46	0.15	0.07	0.13	0.14	0.01	0.09	0.04	0.01
LOI	2.31	1.75	1.46	2.26	3.72	5.17	1.96	3.32	1.94	4.83	4.50	0.65	2.86	1.78	0.64	1.96
Total	100.52	100.67	99.70	99.32	100.39	99.98	98.87	99.65	100.40	99.93	100.35	99.51	100.17	100.17	101.68	99.74
Ba	1180	980	850	1810	894	430	520	1100	340	420	380	1270	1340	550	1250	1060
Rb	59	137	88	94	61	130	37	68	51	148	61	112	136	96	130	196
Sr	159	80	180	117	540	80	460	107	436	194	302	68	14	263	116	99
Y	45	12	21	21	19	31	20	57	29	22	23	38	48	26	19	26
Zr	232	114	133	162	84	118	155	252	154	101	180	287	113	248	178	106
Nb	9.6	5.7	7	8.3	9.3	4.5	4.6	20	3.4	6.6	3.6	10.6	16.1	8	5.7	9.3
Zn	72	27	32	24	78	119	87	107	63	37	45	24	36	30	27	24
Cu	7	2	2	7	59	9	18	60	28	14	31	8	3	10	91	8
Ni	10	5	8	6	117	6	52	7	17	5	16	13	6	8	5	4
V	57	16	10	18	224	150	186	247	134	79	105	54	8	47	19	10
Cr	41	60	137	65	450	55	402	52	80	52	101	310	101	62	5	53
Sc	16	4	5	4.3	30	25	23	28	17	14	14	12	10	9	5	4
Co	11	3	2	5	36	18	23	32	18	9	14	7	4	9	2	3
La	32	29	29	51	19	21	17	33	16	20	16	31	26	22	25	28
Ce	73	63	59	98	40	51	38	73	38	42	37	70	51	50	49	62
Nd	40	35.6	22	28.9	21	29	19	44	22	11.4	20	36	22.1	26	20.1	27
Sm	9.2	5.6	3.4	4.4	4.38	6.7	4	10.6	5.35	2.2	4.39	7	4.8	5.57	3.1	4.5
Eu	2.2	0.7	0.5	0.8	1.3	1.9	1.2	2.4	1.14	0.9	0.99	1.3	0.5	1	0.6	0.7
Gd	8.3	2.9	2.8	3.8	3.88	6.1	3.7	9.7	4.78	3.7	3.77	6.1	5.4	4.59	2.9	4
Dy	7.8	2.3	3.1	3.5	3.19	5.7	3.5	9.3	4.74	3.6	3.82	6.8	7	4.65	3.3	4.5
Ho	1.6	0.5	0.7	0.8	0.67	1.1	0.7	1.9	0.94	0.7	0.8	1.6	1.7	0.98	0.7	1
Er	4.6	1.4	1.9	2.2	1.85	3.1	2.1	5	2.69	1.9	2.21	4.3	5.7	2.85	2.1	2.9
Yb	4.7	1.5	1.9	2.2	1.87	3.1	2	5.1	2.84	1.9	2.24	4.3	5.7	2.9	2.1	2.9
Lu	0.7	0.2	0.3	0.4	0.29	0.5	0.3	0.8	0.43	0.3	0.34	0.7	0.9	0.45	0.3	0.4
UTM	4909217N 279512E	*	4871270N 271543E	4772500N 281800E	*	4925659N 718368E	*	*	*	4778000N 693000E	*	*	4954480N 275560E	4972324N 303012E	4920022N 712672E	4934322N 273637E

* UTM coordinates given in tables 1 and 2.

(table 4 continued)

	Cretaceous						Eocene									
Sample	170495-2	170495-1	200495-2	210495-2	200495-5	011294-2	011294-3	180395-3	200395-2	190395-4	220395-1	180395-2	200395-1	130395-1	180395-1	120395-1
SiO2	75.04	75.82	75.95	76.50	76.76	77.04	48.98	53.61	54.33	56.95	63.60	68.70	70.78	74.37	75.78	76.26
TiO2	0.18	0.09	0.12	0.16	0.18	0.18	3.33	1.00	1.24	0.86	0.87	0.24	0.25	0.09	0.09	0.07
Al2O3	12.69	13.07	11.36	12.07	11.81	11.96	15.34	15.86	16.69	16.98	13.72	13.18	13.76	12.27	12.30	10.58
Fe2O3	0.75	0.95	0.94	1.07	0.95	1.76	2.76	4.45	5.14	1.33	7.08	2.23	0.83	1.08	0.64	0.37
FeO	1.56	0.44	0.36	0.12	0.60	0.10	9.16	3.88	3.28	5.88	0.28	0.74	1.84	0.26	0.92	0.84
MnO	0.07	0.04	0.02	0.04	0.03	0.03	0.16	0.16	0.15	0.10	0.07	0.08	0.03	0.04	0.06	0.03
MgO	0.39	0.25	0.29	0.36	0.27	0.21	6.55	3.98	2.78	3.73	1.18	1.25	1.37	0.17	0.86	0.72
CaO	1.49	0.28	1.11	0.67	0.29	0.10	7.86	6.19	5.51	2.41	2.21	2.39	0.89	1.73	1.13	1.29
Na2O	4.20	3.95	1.09	3.32	1.41	4.33	3.69	3.13	3.45	2.38	4.95	1.06	2.62	2.18	0.09	0.91
K2O	3.10	3.72	6.15	4.03	6.67	3.53	0.95	0.95	2.03	2.23	1.66	3.49	4.10	4.01	3.14	5.12
P2O5	0.01	0.01	0.01	0.02	0.02	0.02	0.47	0.17	0.19	0.14	0.15	0.04	0.05	0.01	0.01	0.01
LOI	0.99	0.90	2.27	1.86	1.20	0.61	2.35	6.29	4.87	6.58	3.73	5.67	2.64	3.36	4.15	3.37
Total	100.47	99.52	99.67	100.22	100.19	99.87	99.60	99.67	99.66	99.57	99.50	99.07	99.16	99.57	99.17	99.57
Ba	840	410	770	536	1760	860	285	372	420	395	490	500	1340	1350	710	880
Rb	106	167	192	117	157	111	15	28	89	69	0.5	129	130	98	113	142
Sr	100	70	122	97	76	107	630	226	198	107	750	114	129	48	34	193
Y	47	36	28	13	18	57	31	26	32	25	19	28	28	27	27	21
Zr	241	83	150	101	120	252	229	122	168	156	129	230	177	197	113	88
Nb	10.2	12.7	8.3	11.8	5	9.3	28	9	7.3	11.8	7.5	11.1	8.9	8.3	7.8	7.1
Zn	58	15	21	23	20	107	150	90	89	41	54	42	28	28	29	16
Cu	3	7	8	3	6	4	30	35	24	15	11	6	6	5	5	8
Ni	5	8	8	4	7	5	66	28	8	9	7	5	4	2	5	5
V	8	9	10	11	12	9	235	165	186	147	82	20	22	10	12	12
Cr	84	200	53	58	156	27	366	163	83	58	77	55	128	70	74	124
Sc	16	7	4	3	4	7	19	26	22	22	12	6.7	7	3.5	4.5	3.5
Co	2	2	2	2	3	3	53	23	23	25	15	4	4	4	4	4
La	29	9	28	28	24	30	24	17	21	24	22	42	43	48	44	30
Ce	65	43	62	55	46	63	56	38	45	50	48	90	85	95	87	63
Nd	35	7	26	18	16	30	34	20	24	24	25	38	36	40	33.6	26
Sm	7.98	1.21	4.84	3.02	2.46	5.92	8.4	4.6	5.2	4.4	4.87	6.7	6.9	6.8	6.4	5.28
Eu	1.49	0.01	0.72	0.39	0.41	0.73	2.4	1.3	1.5	1.1	1.31	1.03	1.1	0.9	0.9	0.57
Gd	7.36	2.09	4.06	2.14	2.56	5.7	8	4.3	5.1	4.2	3.79	5.52	5.6	5.1	5.2	4.1
Dy	8.15	5.09	4.38	1.9	3	7.02	6.4	4.6	5.3	4.3	3.5	5.32	5.1	4.6	4.7	3.37
Ho	1.78	1.33	1	0.41	0.65	1.55	1	0.9	1.2	0.9	0.72	0.98	1	0.9	0.9	0.72
Er	4.99	4.63	3	1.16	1.92	4.5	2.3	2.7	3.2	2.6	2.05	2.75	2.8	2.5	2.6	2.05
Yb	5.32	4.75	2.87	1.22	1.86	4.6	2.1	2.7	3.2	2.5	2.04	2.62	2.7	2.5	2.5	2.03
Lu	0.82	0.72	0.44	0.18	0.3	0.7	0.3	0.4	0.5	0.4	0.32	0.43	0.4	0.4	0.4	0.33
UTM	4939502N 706540E	*	4933579N 275348E	*	4954200N 275300E	*	*	4757466N 681644E	4765865N 681283E	4760521N 680020E	4773000N 284000E	4757466N 681664E	4766348N 680852E	4784000N 699800E	*	4777920N 691120E

TABLE 5. Sr-Nd ISOTOPE DATA FOR REPRESENTATIVE VOLCANIC ROCKS AND RELATED GRANITOID ROCKS.

Sample	Age (Ma)	Rock type	Rb	Sr	Sm	Nd	$^{87}Sr/^{86}Sr$	$^{143}Nd/^{144}Nd$	Sri	Ndi	εNd	T_{DM} (Ga)
Northern Magmatic Domain												
011294-3	49	Olivine basalt	15	630	8,4	0,34	0,704016	0,512874	0,70397	0,512826	4,9	0,5
170495-1	74	Rhyolitic tuff	164	63	2,4	9,1	0,716621	0,5126	0,70699	0,512524	0,4	1,2
011294-1	75	Basaltic andesite	68	107	10,6	0,44	0,707678	0,51262	0,70578	0,512548	0,1	1
200495-2	80	Rhyolitic tuff	106	107	4,6	22,8	0,713808	0,512513	0,71063	0,512448	-1,7	0,9
200495-6	80	Dacitic tuff	136	14	4,8	22,1	0,708868	0,512582	0,70595	0,512514	-0,4	0,9
210495-3	82	Andesite	51	436	5,4	0,22	0,705194	0,512726	0,70469	0,512647	2,2	0,8
210495-2	96	Rhyolitic tuff	66	89	3,5	23,2	0,708604	0,512811	0,70578	0,512753	4,7	0,4
190495-1	99	Basalt	130	80	6,7	29	0,705853	0,512613	0,70504	0,512522	0,2	0,9
190495-6	100	Rhyolitic tuff	130	116	3,1	20,1	0,711718	0,512582	0,70726	0,512511	0	0,9
210495-4	113	Olivine basalt	61	540	4,4	21	0,705194	0,512652	0,7047	0,512559	1,3	0,7
Southern Magmatic Domain												
180395-3	47	Basaltic andesite	28	226	4,6	20	0,708009	0,512464	0,70778	0,512421	-3,1	0,8
180395-1	47	Rhyolitic tuff	113	34	6,4	33,6	0,736315	0,512376	0,72837	0,512341	-4,6	1
120395-4	47	Rhyolitic tuff	135	233	4,1	20,2	0,713329	0,512373	0,71224	0,512335	-4,7	1,1
120395-7	92	Dacitic tuff	148	194	2,2	11,4	0,708231	0,512497	0,70545	0,512426	-1,8	0,9
180495-3	129	Rhyolitic tuff	137	80	5,6	35,6	0,720009	0,512426	0,70892	0,512346	-2,5	0,8
120395-10	160	Rhyolitic tuff	94	117	4,4	28,9	0,714405	0,512362	0,70927	0,512265	-3,3	0,9
140395-1*	158	Tonalite	78	307	3,7	15,6			0,70825	0,512257	-3,7	1,4
190395-3*	158	Tonalite	59	218	4,2	18,4			0,70686	0,512304	-2,9	1

*Samples from the El Faldeo granitoids; data of Sri, Ndi and εNd were taken from Parada *et al.* (1997).
Initial $^{87}Sr/^{86}Sr$ and εNd values are calculated at the assumed age with the following ratios: $^{87}Rb/^{86}Sr_{BE}$ = 0.0816, $^{87}Sr/^{86}Sr_{BE}$ = 0.7045, $^{147}Sm/^{144}Nd_{CHUR}$ = 0.1967, $^{143}Nd/^{144}Nd_{CHUR}$ = 0.51264. Model Nd ages (T_{DM}) are calculated with reference to the depleted mantle reservoir using parameters of normalization after Michard et al. (1985). The El Faldeo granitoid rocks are located at 47°27'S-72°30'W.

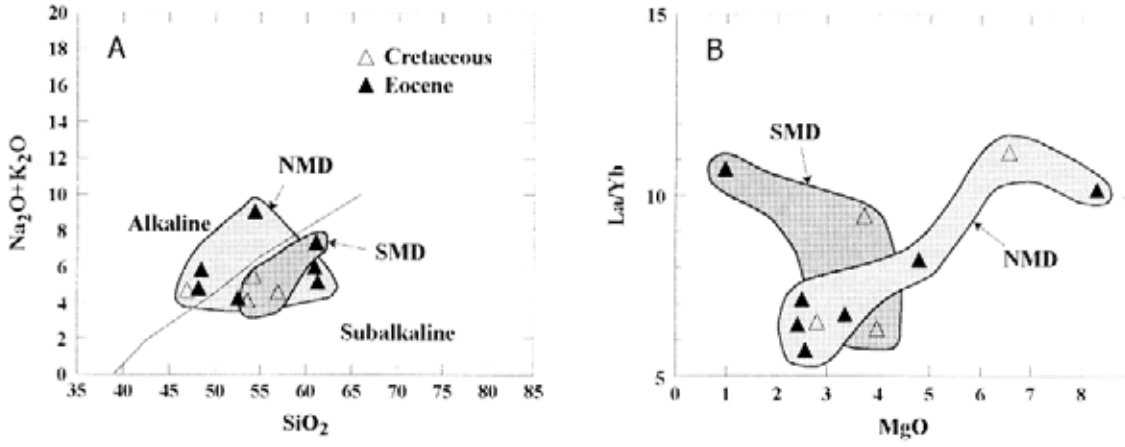

FIG. 5. **A-** alkalies *versus* SiO_2, and **B-** La/Yb *versus* MgO plots for mafic and intermediate volcanic rocks of the Northern and Southern magmatic domains.

the trace element composition of the Eocene Balmaceda basalts as resulting from an asthenospheric mantle source in a back-arc extensional regime, which in turn would have originated from arrested subduction as a consequence of a contemporaneous oceanic ridge-trench collision (cf. Ramos and Kay, 1992).

The intermediate to acidic tuffs and lavas (>63% SiO_2) of the NMD have slightly higher alumina and alkali contents, and lower La/Yb and Sm/Yb ratios than their SMD equivalents (Fig. 8). They exhibit a broad spectrum of Sr-Nd isotopic values. Their initial $^{87}Sr/^{86}Sr$ ratios range from 0.70401 to 0.71063,

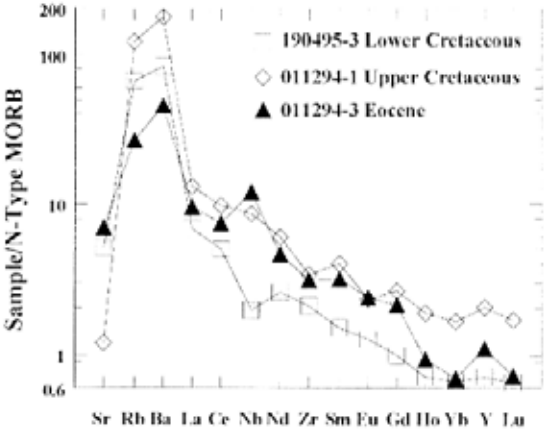

FIG. 6. Trace element abundance patterns, normalized to N-MORB for three representative mafic rocks of Lower Cretaceous, Upper Cretaceous and Eocene age of the Northern Magmatic Domain. Normalizing values are from Sun and McDonough (1989).

and the εNd varies from -1.7 to + 4.7 (Table 5). Compared with the basalts, one of the analyzed felsic samples is by far, isotopically more enriched (Sr_i: 0.71063; εNd: -1.7) whereas the remaining felsic samples are rather similar (Fig. 7), which is compatible with a small degree of crustal participation.

SOUTHERN MAGMATIC DOMAIN (SMD)

Unlike the mafic rocks of the NMD, the analyzed basalts, basaltic andesites and andesites from the SMD have a subalkaline character irrespective of age (Fig. 5a). The analyzed samples of basaltic andesites and andesite have initial $^{87}Sr/^{86}Sr$ ratios of 0.70545 and 0.70778, and εNd of -3.1 and -1.8 (Table 5). Compared with the isotopic characteristics of the NMD mafic rocks, these isotopic values have lithospheric signature, although the authors cannot determine the magnitude of the contribution of the lithospheric mantle and the continental crust on the isotopic features. Moreover, the possibility exists that the isotopic values of the SMD mafic and intermediate rocks could be mainly due to crustal contamination of magmas derived from asthenospheric mantle like those of the NMD basalts. If this was the case, a relatively large degree of contamination from the metamorphic basement is required to change up to 8 εNd units of a NMD depleted basaltic magma and consequently, more significant effects in the whole-rock composition would be expected.

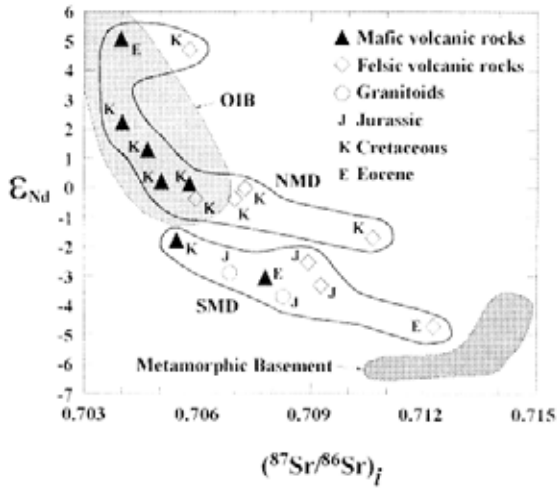

FIG. 7. εNd initial $^{87}Sr/^{86}Sr$ for rocks from the Northern and Southern magmatic domains in comparision with Ocean Island Basalts (OIB) and rocks of the metamorphic basement. The field of OIB is taken from Feuerbach *et al.* (1993); the field of metamorphic basement was obtained from data of Weaver *et al.* (1990). Sample 180395-1 was not plotted because it has a very anomalous high initial strontium value, probably due to carbonates replacing feldspar.

The felsic volcanic rocks of the SMD (with the exception of the highly Sr radiogenic sample 180395-1) have slightly higher initial $^{87}Sr/^{86}Sr$ ratios (0.70892 to 0.71224) and definitively lower εNd values (-2.5 to -4.7) than the equivalent rocks of the NMD, suggesting a larger crustal contribution in the magma sources. In addition, the slightly higher La/Yb and Sm/Yb ratios of the SMD felsic volcanic rocks (Fig. 8) may reflect differences in the residual mineralogy of the respective sources, such as the presence of garnet and/or amphibole in the SMD crustal source.

It is possible to recognize metasedimentary rocks of the metamorphic basement as a source component of the felsic volcanic rocks of the SMD. In fact, Sr-Nd isotopic values for three basement samples calculated at 150 Ma (taken from Weaver *et al.*, 1990), plot close to the felsic rocks of the SMD (Fig. 7). The similarities between the Nd model ages (T_{DM}) of the basement rocks (1.5 - 1.1 Ga), calculated from the published Nd isotope data (Weaver *et al.*, 1990), and those of the rhyolites of the SMD (1.4 - 0.8 Ga; Table 5), support the mentioned genetic link between the two types of rocks. Influence of lower crustal basement has been also invoked to explain the enriched Sr-Nd isotopic compositions of Early Cretaceous granitoids of the western margin of the Patagonian Batholith at the same latitudes of the studied area (Pankhurst *et al.*, 1999). However, the Early Cretaceous granitoids are located both north and south of the limit between the NMD and SMD. At present the authors cannot precise if this situation is an indication of different crustal components of the magma sources in the arc and back-arc regions or is that later tectonic events (*e.g.*, those associated with the dextral LOFZ) has displaced the Early Cretaceous granitoids from its original position.

Consistent with a crustal participation in the origin of the SMD rocks are the crustal Sr-Nd signatures obtained in tonalite plutons (initial $^{87}Sr/^{86}Sr$ = 0.707 and 0.708; εNd = -2.9 and -3.7) of the Jurassic El Faldeo polymetallic district located in the SMD near Cochrane. It is interesting to note that the radiogenic lead isotopic ratios ($^{206}Pb/^{204}Pb$ = 19.006-19.236 and $^{207}Pb/^{204}Pb$ = 15.688-15.703) of some galenas from the El Faldeo district define a field close to the average upper crust growth curve (Parada *et al.*, 1997). Rocks from the metamorphic basement have been considered as a prime candidate for the crustal source components of these galenas (Parada *et al.*, 1997), which differ from the mantle-derived galenas of the Cretaceous El Toqui Pb-Zn district in the NMD (Puig, 1988). On a regional scale, the involvement of the Paleozoic metamorphic basement as a source of lead has been also recorded in other ore deposits of the SMD (Townley, 1996).

DISCUSSION: INFERENCES FOR MANTLE-CRUST RELATIONS

One of the striking features of the Patagonian volcanism in Chile and Argentina is the presence of flood basalts, such as those of the Pliocene Meseta Buenos Aires and Eocene Posadas, which have been considered as a back-arc testimony of ridge collisions (Ramos and Kay, 1992). For example, collision of different segments of the Antarctica-Nazca Ridge during the Late Miocene-Pliocene would have been responsible for the coeval flood basalt formation as a result of melting associated

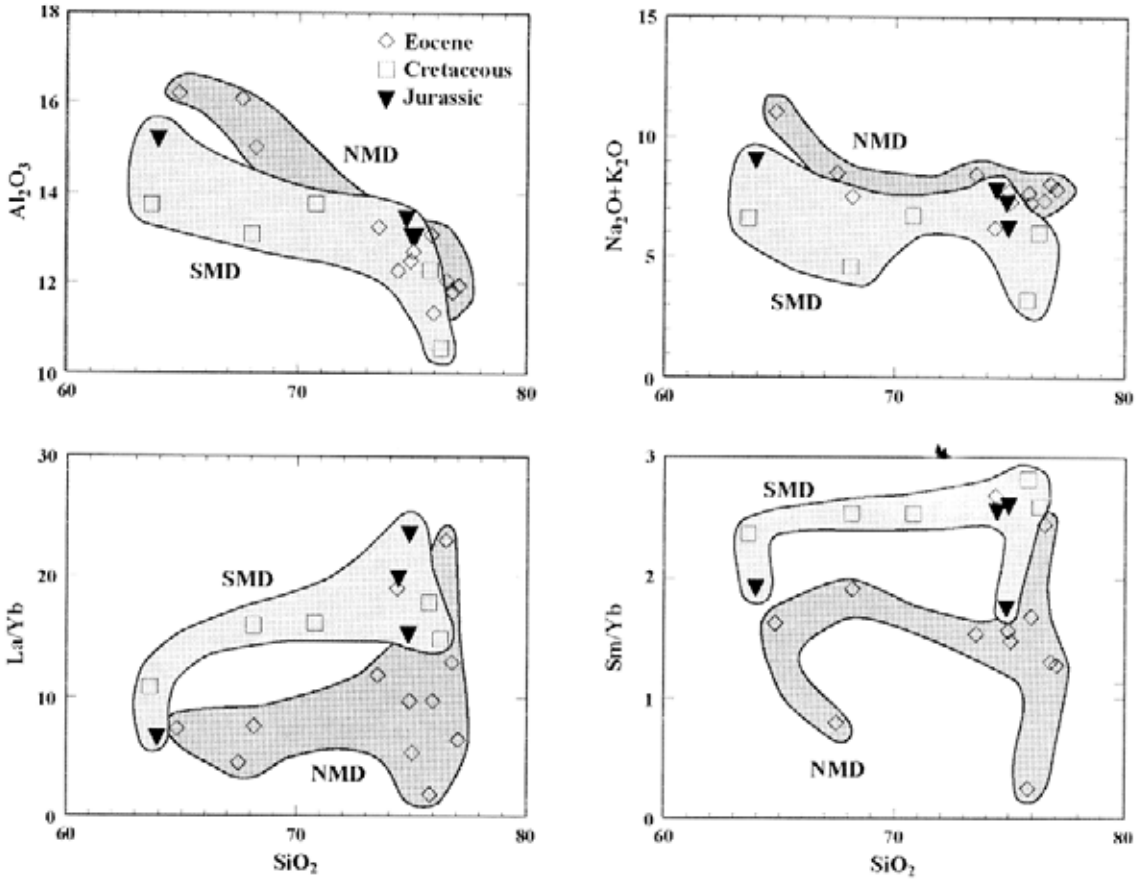

FIG. 8. Selected variation diagrams for felsic volcanic rocks of the Northern and Southern magmatic domains.

with the slab window. This situation explains why this basaltic magmatism is spatially restricted to the gap in the arc between the Southern Volcanic Zone and the Austral Volcanic Zone, between 46°30'S and 49°S (Ramos and Kay, 1992), and why it was formed in a short time interval (Daniel, 1996).

Back-arc basalts are also widespread in the Chilean Patagonia distributed along the studied area as components of pre-Miocene bimodal sequences. In fact, flat-lying basalts are recognized in the Divisadero and Ñirehuao Formations as well as in the Eocene Balmaceda volcanic rocks. However, the model of slab window-related magmatism appears to be unsustainable in all these cases. The well-known genetic association of extension and basaltic volcanism (White *et al.*, 1987; White and McKenzie, 1989; Fitton *et al.*, 1991; Feuerbach *et al.*, 1993) seems inevitable in the case of the Cretaceous event. Extensional tectonics implies stretching and thinning of the lithosphere and upwelling of the hot asthenosphere that favour its decompression melting and crustal fusion. As the volume of the basaltic magmatism depends, among other factors, on the amount of lithospheric extension (White and McKenzie, 1989; Fitton *et al.*, 1991), the Cretaceous event, dominated by felsic volcanic rocks, probably developed in a moderately thinned lithosphere. Compared with the SMD, a larger amount of extension and crustal thinning in the NMD is deduced from the more relevant development of the Lower Cretaceous basin and the smaller La/Yb ratios of the felsic rocks (Fig. 8), which are an indirect indicator of the relative tickness of the lithosphere (cf. Ellam, 1992).

As a general feature, synextensional mafic volcanic rocks may provide information about the subcontinental mantle concerning their chemical and isotopic compositions. The lithospheric mantle much like the continental crust is enriched in incompatible elements and Sr-Nd isotopes relative to the

asthenospheric mantle. Despite the small number of analyzed mafic rocks, the geochemical and isotopic differences established for the two domains, suggest that, at least during the Cretaceous-Eocene interval, the boundary between them would correspond to a boundary of back-arc segments with asthenospheric participation in the source beneath the NMD and lithospheric-dominated source beneath the SMD. Decompression partial melting of asthenospheric material requires mantle upwelling, which in turn may cause crustal extension. In the NMD, where the extension was greater, the asthenospheric upwelling would have reached a shallower depth, provided that sufficient forces existed to cause remotion of the lithosphere, and that enough heat was available as to disturb the crustal thermal gradient. It is reasonable to speculate that the thermal gradient in the NMD would have been high if one considers that the Mesozoic and Cenozoic volcanic sequences in the NMD were affected by low-grade metamorphism with temperatures in the range of 120 to 340°C and pressure below 2 kbars (Aguirre *et al.*, 1997). These authors have also shown that the metamorphism of the Cretaceous rocks developed under a rising thermal gradient, which is consistent with the mechanism of thermally driven subsidence that have been invoked for the development of the Lower Cretaceous Aysén basin (Bell and Suárez, 1997).

The causes of asthenospheric mantle upwelling and subsequent extension in the NMD can be attributed to several mechanisms, *e.g.*, subduction-induced mantle upwelling in a back-arc setting, lithospheric delamination or a mantle plume. Processes like these are difficult to test, however, whatever the process it should be one of long duration. The authors suggest mantle upwelling as a feasible mechanism to explain the extension in the NMD during the Cretaceous. According to Liu and Shen (1998) extensional forces would act for a long time (> 20 m.y.) with an active asthenospheric upwelling such as in a mantle plume where the temperature is maintained by convection.

CONCLUSIONS

Three pre-Miocene back-arc volcanic events are defined in the Aysén region of Chilean Patagonia: Middle Jurassic - Early Cretaceous, Cretaceous and Eocene. These events roughly correlate with those recognized earlier in the Patagonian Batholith (Pankhurst *et al.*, 1999). Likewise in the Cretaceous plutonic event of the Patagonian Batholith, the Cretaceous back-arc volcanic event is the most intensive as is suggested by the extensive distribution of its products. It is interesting to note the overlap between the ages of the Ñirehuao and Divisadero formations, suggesting that they represent a single Cretaceous volcanic event.

The distinct compositional characteristics of the mafic rocks of the two domains defined here, are attributed to different contributions of the asthenosphere and lithosphere (mantle and/or crust) as a source of the magmas. The crustal participation is more evident in the origin of the felsic volcanic rocks. Particularly relevant is the participation of metasedimentary rocks of the Paleozoic metamorphic basement in the origin of the felsic rocks of the SMD.

ACKNOWLEDGEMENTS

This study was financed by FONDEF Project MI-15. The authors are grateful to L. Aguirre and J.P. Le Roux (Universidad de Chile) for correcting early versions of the manuscript. The authors also acknowledge helpful reviews by T.R. Riley (British Antarctic Survey), A. Demant (Université d'Aix-Marseille) and M. Suárez (Sernageomin).

REFERENCES

Aguirre, L.; Cortés, J.; Morata, D.; Hervé, F. 1997. Low-grade metamorphism of Mesozoic and Cenozoic volcanic sequences of Patagonia, Chile (43-46°S). *Revista Geológica de Chile*, Vol. 24, No. 2, p. 187-201.

Baker, P.E.; Rea, W.J.; Skarmeta, J.; Caminos, R.; Rex, D.C. 1981. Igneous history of the Andean Cordillera and Patagonian Plateau around latitude 46ºS. *Philosophical Transactions of the Royal Society of London Series*, Vol. A303, p. 105-149.

Bartholomew, D.S. 1984. Geology and geochemistry of the Patagonian batholith (45º - 46º S). Chile. Ph.D. Thesis (Unpublished), *University of Leicester*, 195 p.

Bartholomew, D.S.; Tarney, J. 1984. Crustal extension in the southern Andes (45 - 46° S). *In* Volcanic Processes in Marginal Basins (Kokelaar, B.P.; Howells, M.F.; Roach, R.A.; editors). *Geological Society of London, Special Publication*, No. 16, p. 195-205. London.

Bell, C.M.; Suárez, M. 1997. The Lower Cretaceous Apeleg Formation of the Aisén basin, southern Chile. Tidal sandbar deposits of an epicontinental sea. *Revista Geológica de Chile*, Vol. 24, No. 2, p. 203-225.

Bell, C.M.; Suárez, M. 2000. The Río Lácteo Formation of Southern Chile. Late Paleozoic orogeny in the Andes of southernmost South America. *Journal of South American Earth Sciences*, Vol. 13, p. 133-145.

Belmar, M. 1996. Geologia de los cuadrángulos Balmaceda y Cerro Farellón Norte, Región de Aisén. Memoria de Título (Unpublished), *Universidad de Chile, Departamento de Geología*, 83 p.

Bruce, R.M.; Nelson, E.P.; Weaver, S.G.; Lux, D.R. 1991. Temporal and spatial variation in the southern Patagonian Batholith; Constraints on magmatic arc development. *In* Andean Magmatism and its Tectonic Setting (Harmon, R.S.; Rapela, C.W.; editors). *Geological Society of America*, Vol. 265, *Special Paper*, p. 1-12.

Butler, R.F.; Hervé, F.; Munizaga, F.; Beck, M.E.; Burmester, R.F.; Oviedo, E. 1991. Paleomagnetism of the Patagonian Plateau basalts, southern Chile and Argentina. *Journal of Geophysical Research*, Vol. 96, p. 6023-6034.

Cande, S.C.; Leslie, R.B. 1986. Late Cenozoic tectonics of the southern Chile trench. *Journal of Geophysical Research*, Vol. 91, p. 471-496.

Cembrano, J.; Hervé, F. 1993. The Liquiñe-Ofqui Fault Zone: a major Cenozoic strike slip duplex in the southern Andes. *In Second International Symposium on Andean Geodynamics, No. 2, Actas*, p. 175-178. Oxford, England.

Charrier, R.; Linares, E.; Niemeyer, H.; Skármeta, J. 1979. K-Ar ages of basalt flows of Meseta Buenos Aires in southern Chile and their relation to the southeast Pacific triple junction. *Geology*, Vol. 7, p. 436-439.

Daniel, A.J. 1996. The geodynamics of spreading centre subduction in southern Chile. Ph.D. Thesis (Unpublished), *University of Liverpool*, 181 p.

Demant, A.; Hervé, F.; Pankhurst, R.J.; Suárez, M. 1996. Geochemistry of Early Tertiary back-arc basalts from Aysén, southern Chile (44-46°S): geodynamic implications. *In Third International Symposium on Andean Geodynamics, No. 3, Actas*, p. 555-558. St. Malo, France.

Drake, R.E.; Vergara, M.; Munizaga, F.; Vicente, J.C. 1982. Geochronology of Mesozoic-Cenozoic magmatism in central Chile, Lat 31°- 36° S. *Earth-Science Reviews*, Vol. 18, p. 353-363.

Duffield, W.A.; Dalrymple, G.B. 1990. The Taylor Creek rhyolite of New Mexico: A rapidly emplaced field of lava domes and flows. *Bulletin of Volcanology*, Vol. 52, p. 475-487.

Ellam, R.M. 1992. Lithospheric thickness as a control on basalt geochemistry. *Geology*, Vol. 20, p. 153-156.

Féraud, G.; Alric, V.; Fornari, M.; Bertrand, H.; Haller, M. 1999. ^{40}Ar-^{39}Ar dating of the Jurassic volcanic province of Patagonia: migrating magmatism related to Gondwana break-up and subduction. *Earth and Planetary Science Letters*, Vol. 172, p. 83-96.

Feuerbach, D.L.; Smith, E.I.; Walker, J.D.; Tangeman, J.A. 1993. The role of the mantle during crustal extension: constraints from geochemistry of volcanic rocks in the Lake Mead area, Nevada and Arizona. *Geological Society of America, Bulletin*, Vol. 105, p. 1561-1575.

Fitton, J.G.; James, D.; Leeman, W.P. 1991. Basic magmatism associated with Late Cenozoic extension in the western United States: compositional variations in space and time. *Journal of Geophysical Research*, Vol. 96, p. 13693-13711.

Flint, S.S.; Prior, D.J.; Agar, S.M.; Turner, P. 1994. Stratigraphic and structural evolution of the Tertiary Cosmelli Basin and its relationship to the Chile triple junction. *Journal of the Geological Society of London*, Vol. 151, p. 251-268.

Halpern, M.; Fuenzalida, R. 1978. Rubidium-Strontium geochronology of a transect of the Chilean Andes between latitudes 45° and 46° S. *Earth and Planetary Science Letters*, Vol. 41, p. 60-66.

Hervé, F. 1984. Rejuvenecimiento de edades radiométricas y el sistema de fallas Liquiñe-Ofqui. *Comunicaciones*, Vol. 35, p. 107-116.

Hervé, F.; Godoy, E.; Parada, M.A.; Ramos, V.; Rapela, C.W.; Mpodozis, C.; Davidson, J. 1987. A general view on the Chilean-Argentine Andes with emphasis on their early history. *In* Circum-Pacific Orogenic belts and the Evolution of the Pacific Ocean Basin (Monger, J.W.H.; Francheteau, J.; editors). *American Geophysical Union Geodynamic Series*, Vol. 18, p. 97-114.

Liu, M.; Shen, Y. 1998. Crustal collapse, mantle upwelling and Cenozoic extension in the North American Cordillera. *Tectonics*, Vol. 17, p. 311-321.

Michard, A.; Gurriet, P.; Soudant, M.; Albarede, F. 1985. Nd isotopes in French phanerozoic shales: external vs internal aspects of crustal evolution. *Geochimica et Cosmochimica Acta*, Vol. 49, p. 601-610.

Nelson, E.; Forsythe, R.; Diemer, J.; Allen, M.; Urbina, O. 1993. Taitao ophiolite: a ridge collision ophiolite in the forearc of southern Chile (46°S). *Revista Geológica de Chile*, Vol. 20, p. 137-165.

Niemeyer, H. 1975. Geología de la región comprendida entre el lago General Carrera y el río Chacabuco, Provincia de Aysén, Chile. Memoria de Título (Unpublished), *Universidad de Chile, Departamento de Geología*, 309 p.

Niemeyer, H.; Skármeta, J.; Fuenzalida, R.; Espinosa, W. 1984. Hojas Península Taitao y Puerto Aisén, Región de Aysén del General Carlos Ibáñez del Campo. *Servicio Nacional de Geología y Minería, Carta Geológica de Chile*, No. 60-61.

Palacios, C.; Parada, M.A.; Lahsen, A. 1997. Upper Jurassic mineralization in El Faldeo district, Chilean Patagonia. *Geologische Rundschau*, Vol. 86, p. 132-140.

Pankhurst, R.J.; Hervé, F. 1994. Granitoid age distribution and emplacement control in the North Patagonian Batholith in Aysén (44° - 47°S). *In Congreso Geológico Chileno, No. 7, Actas*, Vol. 2, p. 1409-1413. Concepción.

Pankhurst, R.J.; Weaver, S.D.; Hervé, F.; Larrondo, P. 1999. Mesozoic-Cenozoic evolution of the North Patagonian Batholith in Aysén, southern Chile. *Journal of the Geological Society of London*, Vol. 156, p. 673-694.

Pankhurst, R.J.; Riley, T.R.; Fanning, C.M.; Kelley, S.P. 2000. Episodic silicic volcanism in Patagonia and the Antarctic Peninsula: chronology of magmatism associated with the break-up of Gondwana. *Journal of Petrology*, Vol. 41, p. 605-625.

Parada, M.A.; Rivano, S.; Sepúlveda, P.; Hervé, F.; Puig, A.; Munizaga, F.; Brook, M.; Pankhurst, R.J.; Snelling, N. 1988. Mesozoic and Cenozoic plutonic development in the Andes of central Chile (30°30'-32°30' S). *Journal of South American Earth Sciences*, Vol. 1, p. 249-260.

Parada, M.A.; Palacios, C.; Lahsen, A. 1997. Jurassic extensional tectono-magmatism and associated mineralization of the El Faldeo polymetallic district, Chilean Patagonia: geochemical and isotopic evidence of crustal contribution. *Mineralium Deposita*, Vol. 32, p. 547-554.

Pardo-Casas, F.; Molnar, P. 1987. Relative motion of the Nazca (Farallón) and South American plates since Late Cretaceous time. *Tectonics*, Vol. 6, p. 233-248.

Petford, N.; Turner, P. 1993. Geochemistry and paleomagnetism of igneous rocks from the Cosmelli Basin, southern Chile. *In International Symposium on Andean Geodynamics, No. 2, Actas*, p. 433-435. Oxford, England.

Petford, N.; Cheadle, M.; Barreiro, B. 1996. Age and origin of southern Patagonian flood basalts, Chile Chico region (46°45'S). *In International Symposium on Andean Geodynamics, No. 3, Actas*, p. 629-632. St. Malo, France.

Puig, A. 1988. Geologic and metallogenic significance of the isotopic composition of lead in galenas of the Chilean Andes. *Economic Geology*, Vol. 83, p. 843-858.

Ramos, V. 1976. Estratigrafía de los lagos La Plata y Fontana, Provincia de Chubut - República Argentina. *In Congreso Geológico Chileno, No. 1, Actas*, Vol. 1, p. A43-A64. Santiago.

Ramos, V.; Niemeyer, H.; Skármeta, J.; Muñoz, J. 1982. Magmatic evolution of the Austral Patagonian Andes. *Earth Science Reviews*, Vol. 18, p. 411-443.

Ramos, V.; Kay, S.M. 1992. Southern Patagonian plateau basalts and deformation: backarc testimony of ridge collisions. *Tectonophysics*, Vol. 205, p. 261-282.

Skármeta, J.; Charrier, R. 1976. Geología del sector fronterizo de Aysén entre los 45° y 46° de latitud sur, Chile. *In Congreso Geológico Argentino, No. 4, Actas*, Vol. 1, p. 267-286. Bahía Blanca, Argentina.

Suárez, M.; De la Cruz, R. 1997. Cronología magmática de Aysén sur (45°-48°30'L.S.). *In Congreso Geológico Chileno, No. 8, Actas*, Vol. 2, p. 1543-1547. Antofagasta.

Suárez, M.; De la Cruz, R. 2000. Tectonics in the eastern central Patagonian Cordillera (45°30'-47°30'S). *Journal of the Geological Society of London*, Vol. 157, p. 995-1001.

Suárez, M.; De la Cruz, R.; Bell, C.M. 2000. Timing and origin of deformation along the Patagonian fold and thrust belt. *Geological Magazine*, Vol. 137, p. 345-353.

Suárez, M.; De la Cruz, R. 2001. Jurassic to Miocene K-Ar dates from eastern central Patagonian Cordillera plutons, Chile (45°-48° S). *Geological Magazine*, Vol. 138, No. 1, p.53-66.

Sun, S.-s.; McDonough, W.F. 1989. Chemical and isotopic systematics of oceanic basalts: implications for mantle composition and processes. *In* Magmatism in the Ocean Basins (Saunders, A.D.; Norry, M.J.; editors). *Geological Society*, No. 42, Special Publication, p. 313-345. London.

Townley, B. 1996. Ore deposits, tectonics and metallogenesis of the continental Aysén region, Chile. Ph.D. Thesis (Unpublished), *Queen's University*, 246 p.

Weaver, S.G.; Bruce, R.; Nelson, E.P.; Brueckner, H.K.; LeHuray, A.P. 1990. The Patagonian batholith at 48° S latitude, Chile; geochemical and isotopic variations. *In* Plutonism from Antarctica to Alaska (Kay, S.M.; Rapela, C.W.; editors). *Geological Society of America*, Vol. 241, Special Paper, p. 33-50.

White, R.S.; Spence, G.D.; Fowler, S.R.; McKenzie, D.P.; Westbrook, G.K.; Bowen, A.N. 1987. Magmatism at rifted continental margins. *Nature*, Vol. 330, p. 439-444.

White, R.; McKenzie, D. 1989. Magmatism at rift zones: the generation of volcanic continental margins and flood basalts. *Journal of Geophysical Research*, Vol. 94, p. 7685-7729.

Yoshida, K. 1981. Estudio geológico del curso superior del rio Baker, Aysén, Chile. Ph.D. Thesis (Unpublished), *Universidad de Chile, Departamento de Geologia*, 341 p.

Manuscript received: September 26, 2000; accepted: April 2, 2001.